

Stability of plates using rectangular bar cells

Autor(en): **Hrennikoff, A. / Mathew, C.I. / Sen, Rajan**

Objektyp: **Article**

Zeitschrift: **IABSE publications = Mémoires AIPC = IVBH Abhandlungen**

Band (Jahr): **32 (1972)**

PDF erstellt am: **22.07.2024**

Persistenter Link: <https://doi.org/10.5169/seals-24944>

Nutzungsbedingungen

Die ETH-Bibliothek ist Anbieterin der digitalisierten Zeitschriften. Sie besitzt keine Urheberrechte an den Inhalten der Zeitschriften. Die Rechte liegen in der Regel bei den Herausgebern.

Die auf der Plattform e-periodica veröffentlichten Dokumente stehen für nicht-kommerzielle Zwecke in Lehre und Forschung sowie für die private Nutzung frei zur Verfügung. Einzelne Dateien oder Ausdrucke aus diesem Angebot können zusammen mit diesen Nutzungsbedingungen und den korrekten Herkunftsbezeichnungen weitergegeben werden.

Das Veröffentlichen von Bildern in Print- und Online-Publikationen ist nur mit vorheriger Genehmigung der Rechteinhaber erlaubt. Die systematische Speicherung von Teilen des elektronischen Angebots auf anderen Servern bedarf ebenfalls des schriftlichen Einverständnisses der Rechteinhaber.

Haftungsausschluss

Alle Angaben erfolgen ohne Gewähr für Vollständigkeit oder Richtigkeit. Es wird keine Haftung übernommen für Schäden durch die Verwendung von Informationen aus diesem Online-Angebot oder durch das Fehlen von Informationen. Dies gilt auch für Inhalte Dritter, die über dieses Angebot zugänglich sind.

Stability of Plates Using Rectangular Bar Cells

Stabilité de dalles utilisant des éléments de barre rectangulaires

Festigkeit von Platten bei Anwendung rechteckiger Stabelemente

A. HRENNIKOFF

Sc.D., Research Professor Emeritus of
Civil Engineering. The University of British
Columbia, Vancouver B.C., Canada

C. I. MATHEW

M.Sc., (Eng.), Principal, Government
Polytechnic Kalamassery, Kerala,
India

RAJAN SEN

Graduate Student, Dept. of Civil Engineering. The University of British Columbia,
Vancouver B.C., Canada

General Principles

The plate model must be composed of the elements endowed with proper elastic properties, as manifested by their plane stress and flexural stiffness matrices. The plane stress loads are assumed to increase gradually and in unison to the critical value. Once the critical condition has been reached, the model suffers a flexural deformation of a variable magnitude in some definite mode. Both the plane stress and the flexural deformations are considered small. The plane stress condition in the model is assumed to remain constant in the course of buckling and the energy of flexural deformation independent of the plane stress.

As the structure buckles the increment T of its total energy remains zero. This quantity is made up of the energy of deformation U and the potential energy of the loads V .

Thus,
$$T = U + V = 0. \quad (1)$$

With the plane stress being unaffected by buckling, U in this equation equals the flexural energy of the buckled structure with no contribution from the plane stress. The other part of the total energy, $V = -\sum P \epsilon$, is negative. The quantities ϵ are the components of displacements of the points of application of the loads P in the directions of the loads, suffered in the

course of buckling. The quantities U and ϵ depend on the mode of buckling described by the displacements w , θ^x and θ^y of the nodes of the model. The required displacements and with them the critical load are found by minimizing T . Both the bar and the no-bar cells may be used in analysis, the rectangular bar cells being particularly convenient for explicit formulation of the principal steps of the method.

Stability of Bar Cell Model

The model carries a set of in-plane loads P , described as having a unit intensity, and causing stresses S in its bars. As the loading is increased proportionately to the level of critical intensity f , the stresses are increased to fS . Since the structure in the course of buckling is in a state of neutral equilibrium, the virtual work equation is applicable to it. The virtual deformation is considered to be made up of the movements ϵ in the expression for V from the pre-buckling condition to the post-buckling one. These displacements are brought about by flexure of the bars resulting in decreases λ in the lengths of their projections (Fig. 1) unto the plane of the plate.

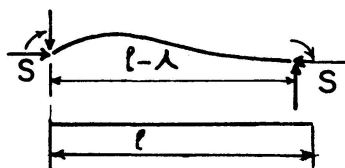


Fig. 1.

Thus,
$$\sum (f P \epsilon) = \sum (f S \lambda). \quad (2)$$

Although the loads P are present only in a few locations, the stresses fS and their λ values exist usually in all bars. The transverse forces and the end moments in the bars do not enter the equation since they are balanced by the oppositely directed forces in the adjacent members. The stresses S are considered positive for compression and negative for tension. The quantity λ always signifies a decrease in length, and is used without a sign.

Eq. (1) thus becomes:
$$T = U - f \sum (S \lambda) = 0. \quad (3)$$

Both the energy of flexural deformation U and the length changes λ are quadratic functions of the flexural nodal displacements, called collectively δ .

Minimizing T ,
$$\frac{\partial U}{\partial \delta} - f \sum \left(S \frac{\partial \lambda}{\partial \delta} \right) = 0. \quad (4)$$

Both terms of this equation are linear functions of the displacements δ .

$$\frac{\partial U}{\partial \delta} = [K]_m \{\delta\} \quad \text{and} \quad \sum \left(S \frac{\partial \lambda}{\partial \delta} \right) [K_s]_m \{\delta\}.$$

$[K]_m$ is the flexural stiffness matrix of the model, assembled from 12×12 stiffness matrices of the individual (rectangular) cells $[K]$. Similarly, $[K_s]_m$ is the stability matrix of the model, and $[K_s]$ – the stability matrix of the individual cell, while $\{\delta\}$ is the column vector of the flexural nodal displacements. The individual terms of $[K_s]$ are $\sum \left(S \frac{\partial^2 \lambda}{\partial \delta_m \partial \delta_n} \right)$, the sums of the products of the stresses S in the bars of the cell and the second derivatives of their λ values taken with regard to the nodal displacements δ_m and δ_n corresponding to the location of the term in the matrix.

Eq. (4) may be written:
$$([K]_m - f[K_s]_m)\{\delta\} = 0. \tag{5}$$

This equation expresses an eigenvalue problem satisfied only by some particular values of f associated with the particular modes of nodal displacements δ . The lowest eigenvalue has the greatest practical importance. At the same time the usual mathematical procedure for solution of equations of this kind produces the highest eigenvalue. This calls for transformation of Eq. (5) by dividing it by $-f$.

Then
$$\left([K_s]_m - \frac{1}{f}[K]_m \right) \{\delta\} = 0. \tag{6}$$

The highest eigenvalue $1/f$ of this equation corresponds to the lowest value of f in Eq. (5).

Rectangular Bar Cell in Stability Analysis

It is convenient to use the plane stress cells of the type shown on Fig. 2. These cells, not described in literature, call for an explanation. The framework of each cell consists of the main system of the side and diagonal bars and the secondary system of the corner bars and the subdivided side bars, joined to the primary at the four corner nodes. The secondary system is not needed when the Poisson's ratio μ equals $1/3$. At the other values of μ it is active only when the cell is subjected to pure shear. In conditions of uniform tension,

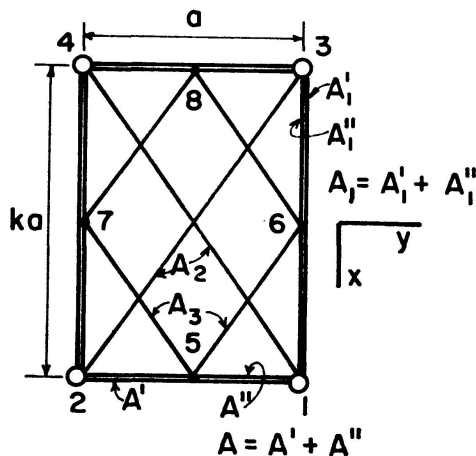


Fig. 2.

compression and shearless bending in the directions of x and y axes the secondary side bars add their areas to the primary, and the corner bars remain inactive.

By subjecting the cell to uniform normal and shearing strains in x and y directions and applying the conditions of equivalence with the plate-prototype [2], the cross-section areas of the bars are found:

$$\begin{aligned}
 A &= A' + A'' = \frac{k^2 - \mu}{2k(1 - \mu^2)} at, \\
 A_1 &= A'_1 + A''_1 = \frac{1 - \mu k^2}{2(1 - \mu^2)} at, \\
 A_2 &= \frac{\mu(k^2 + 1)^{3/2}}{2k(1 - \mu^2)} at.
 \end{aligned}
 \tag{8}$$

The areas of the bars of the secondary system A'' , A''_1 , and A_3 are not required in applications.

The first two columns of the 8×8 stiffness matrix of the cell (i. e., for $u_1 = 1$ and $v_1 = 1$ in Fig. 3) are given in Table 1. The other columns may be obtained by the considerations of symmetry. The matrix is symmetrical about the principal diagonal.

The bar cells used in flexure are of the type introduced by YETTRAM and HUSSEIN [3]. They consist of the side and diagonal bars endowed with flexural

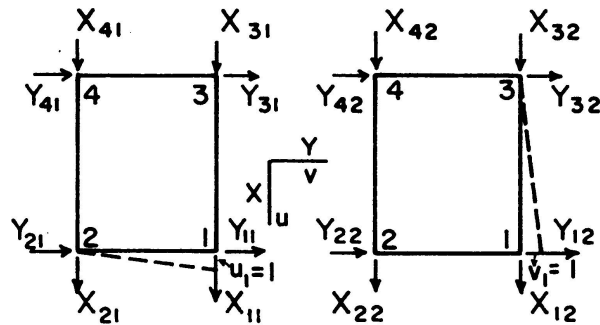


Fig. 3.

Table 1. Stiffness Matrix Terms - Plane Stress - Rectangular Cell

Action 1, $u_1=1$. Fig. 3		Action 2, $v_1=1$. Fig. 3	
$X_{11} = \frac{4 + k^2(1 - 3\mu)}{8k(1 - \mu^2)} Et$	$Y_{11} = \frac{1}{8(1 - \mu)} Et$	$X_{21} = \frac{1}{8(1 - \mu)} Et$	$Y_{12} = \frac{1 - 3\mu + 4k^2}{8k(1 - \mu^2)} Et$
$X_{21} = -\frac{(1 - 3\mu)k}{8(1 - \mu^2)} Et$	$Y_{21} = \frac{1 - 3\mu}{8(1 - \mu^2)} Et$	$X_{22} = \frac{1 - 3\mu}{8(1 - \mu^2)} Et$	$Y_{22} = \frac{1 + \mu - 4k^2}{8k(1 - \mu^2)} Et$
$X_{31} = \frac{-4 + k^2(1 + \mu)}{8k(1 - \mu^2)} Et$	$Y_{31} = \frac{1 - 3\mu}{8(1 - \mu^2)} Et$	$X_{32} = \frac{1 - 3\mu}{8(1 - \mu^2)} Et$	$Y_{32} = \frac{1 - 3\mu}{8k(1 - \mu^2)} Et$
$X_{41} = -\frac{k}{8(1 - \mu)} Et$	$Y_{41} = -\frac{1}{8(1 - \mu)} Et$	$X_{42} = -\frac{1}{8(1 - \mu)} Et$	$Y_{42} = \frac{1}{8k(-\mu^2)} Et$

stiffnesses for bending out of the plane of the plate; their side bars possess also torsional stiffnesses. The 12×12 flexural stiffness matrix is given in Reference [3].

As the nodes of the stressed cell undergo flexural displacements w , θ^x and θ^y , its bars, carrying direct stresses S , undergo shortenings λ of their projected lengths involved in the stability matrix. The actual absence of the corner bars in the flexural cell is treated as the presence of bars of zero flexural stiffness. Such treatment is legitimate because the shape of the deflected bar is independent of the flexural stiffness, which thus may be assumed zero. Possessing no flexural stiffnesses the corner bars do not affect flexure of the side bars to which they connect.

Length Changes λ of the Main Bars

Taking the side bar 2-1 as an example, the shortening of its bent length λ is influenced only by the four corner displacements w_1 , w_2 , θ_1^x , and θ_2^x . The equation of the deflection curve w (Fig. 4) is expressed by the moment-area

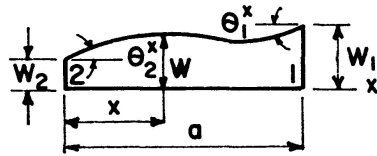


Fig. 4.

relations in terms of the four nodal displacements, and then the quantity

$\lambda_{21} = \frac{1}{2} \int_0^a \left(\frac{dw}{dx} \right)^2 dx$ is evaluated:

$$\begin{aligned} \lambda_{21} = & 0.6 \frac{w_1^2}{a} + 0.6 \frac{w_2^2}{a} + \frac{1}{15} a (\theta_1^x)^2 + \frac{1}{15} a (\theta_2^x)^2 - 1.2 \frac{w_1 w_2}{a} - 0.1 w_1 (\theta_1^x) \\ & - 0.1 w_1 (\theta_2^x) + 0.1 w_2 (\theta_1^x) + 0.1 w_2 (\theta_2^x) - \frac{1}{30} (\theta_1^x) (\theta_2^x) a. \end{aligned} \quad (9)$$

The length change of the half-side bar λ_{25} is found by integration of the same expression over the length $\frac{1}{2} a$

$$\begin{aligned} \lambda_{25} = & 0.3 \frac{w_1^2}{a} + 0.3 \frac{w_2^2}{a} + \frac{17}{960} a (\theta_1^x)^2 + \frac{47}{960} a (\theta_2^x)^2 - 0.6 \frac{w_1 w_2}{a} - \frac{23}{160} w_1 (\theta_1^x) \\ & + \frac{7}{160} w_1 (\theta_2^x) + \frac{23}{160} w_2 (\theta_1^x) - \frac{7}{160} w_2 (\theta_2^x) - \frac{1}{60} a (\theta_1^x) (\theta_2^x). \end{aligned} \quad (10)$$

The λ values of the other side bars and their half lengths may be expressed by similar equations with some other corner displacements replacing the four involved in Eqs. (9) and (10). For example, λ_{13} requires modification of Eq. (9), in which the length a is replaced by ka and the corner movements w_2 , w_1 , θ_2^x and θ_1^x , are changed respectively to w_1 , w_3 , θ_3^y and θ_3^y . The complete corre-

spondence of various λ to λ_{21} and λ_{25} in Eqs. (9) and (10) is presented in Table 2. Strict adherence to the shape of the curve in Fig. 4 determines some of the signs in these relations.

Table 2. Length Changes λ (Eqs. (9) and (10)) – Correspondence of Terms in Different Bars, Fig. 2

Bars (Fig. 2)	2-1 Eq. (9)	3-4	1-3	2-4	2-5 Eq. (10)	5-1	4-7	7-3	1-6	6-3	2-8	8-4
Length	a	a	a	a	a	a	a	a	ka	ka	ka	ka
Node Move-ments	w_1	w_3	w_3	w_4	w_1	w_2	w_3	w_4	w_3	w_1	w_4	w_2
	w_2	w_4	w_1	w_2	w_2	w_1	w_4	w_3	w_1	w_3	w_2	w_4
	θ_1^x	θ_3^x	θ_3^y	θ_4^y	θ_1^x	$-\theta_2^x$	θ_3^x	$-\theta_4^x$	θ_3^y	$-\theta_1^y$	θ_4^y	$-\theta_2^y$
	θ_2^x	θ_4^x	θ_1^y	θ_2^y	θ_2^x	$-\theta_1^y$	θ_4^x	$-\theta_3^y$	θ_1^y	$-\theta_3^x$	θ_2^y	$-\theta_4^y$

The rotations θ_1^x and θ_1^y of the node 1 result in flexural components of rotation $(\theta_1^x - k\theta_1^y)\text{Sin } \alpha$ of the end 1 of the diagonal 4-1, as may be observed by examining the vector diagrams of Fig. 5. Similar relations hold also for the end 4. The end 2 of the diagonal 2-3 undergoes flexure $(\theta_2^x + k\theta_2^y)\text{Sin } \alpha$, and the end 3 behaves similarly. This means that the expression for λ_{41} may be obtained from the Eq. (9) for the side member 2-1 by making in it proper replacements for the length of the member, the end rotations and the numbering of the nodes. Thus

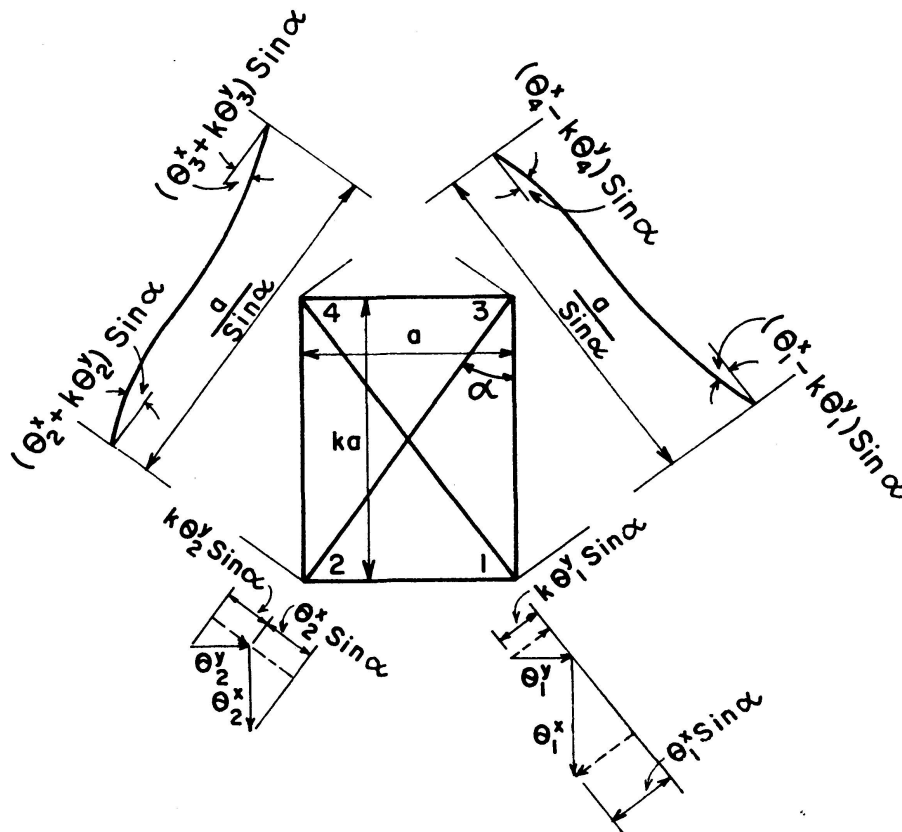


Fig. 5.

$$\begin{aligned}
\lambda_{41} = \text{Sin } \alpha & \left[0.6 \frac{w_1^2}{a} + 0.6 \frac{w_4^2}{a} + \frac{1}{15} a (\theta_1^x)^2 + \frac{k^2}{15} a (\theta_1^y)^2 + \frac{1}{15} a (\theta_4^x)^2 + \frac{k^2}{15} a (\theta_4^y)^2 \right. \\
& - 1.2 \frac{w_1 w_4}{a} - 0.1 w_1 (\theta_1^x) + 0.1 k w_1 (\theta_1^y) - 0.1 w_1 (\theta_4^x) + 0.1 k w_1 (\theta_4^y) \\
& + 0.1 w_4 (\theta_1^x) - 0.1 k w_4 (\theta_1^y) + 0.1 w_4 (\theta_4^x) - 0.1 k w_4 (\theta_4^y) - \frac{2k}{15} a (\theta_1^x) (\theta_1^y) \quad (11) \\
& - \frac{2k}{15} a (\theta_4^x) (\theta_4^y) - \frac{1}{30} a (\theta_1^x) (\theta_4^x) + \frac{k}{30} a (\theta_1^y) (\theta_4^x) + \frac{k}{30} a (\theta_1^x) (\theta_4^y) \\
& \left. - \frac{k^2}{30} a (\theta_1^y) (\theta_4^y) \right].
\end{aligned}$$

The expression for λ_{23} is found from λ_{41} by replacing k by $-k$ and changing the numbers of the nodes 4 and 1 to 2 and 3 respectively.

Length Changes λ of the Corner Bars

Determination of the values λ for the corner bars is explained on the example of λ_{56} . Flexure of this bar is naturally influenced by the transverse displacements and flexural rotations of the end points 5 and 6, which in their turn result from the movements w , θ^x and θ^y of the nodes 1, 2 and 3, the fourth node having no effect on the member 5-6.

The transverse displacements and the flexural corner rotations of the points 5 and 6 are found separately for each of the nine significant nodal displacements of the cell, using the Eq. (9) and the Table 2. With the movements of the ends of the bar 5-6 available, determination of λ_{56} follows the general routine.

$$\begin{aligned}
\lambda_{56} = \text{Sin } \alpha & \left[\frac{3}{16} \frac{w_1^2}{a} + 0.3 \frac{w_2^2}{a} + 0.3 \frac{w_3^2}{a} + \frac{9}{320} a (\theta_1^x)^2 + \frac{17}{960} a (\theta_2^x)^2 + \frac{1}{120} a (\theta_3^x)^2 \right. \\
& + \frac{9k^2}{320} a (\theta_1^y)^2 + \frac{k^2}{120} a (\theta_2^y)^2 + \frac{17k^2}{960} a (\theta_3^y)^2 - \frac{3}{16} \frac{w_1 w_2}{a} - \frac{3}{16} \frac{w_1 w_3}{a} - \frac{3}{32} w_1 (\theta_1^x) \\
& - \frac{1}{32} w_1 (\theta_2^x) - \frac{1}{16} w_1 (\theta_3^x) + \frac{3k}{32} w_1 (\theta_1^y) + \frac{k}{16} w_1 (\theta_2^y) + \frac{k}{32} w_1 (\theta_3^y) - \frac{33}{80} \frac{w_2 w_3}{a} \\
& - \frac{13}{160} w_2 (\theta_1^x) + \frac{23}{160} w_2 (\theta_2^x) + \frac{3}{80} w_2 (\theta_3^x) - \frac{7k}{40} w_2 (\theta_1^y) - \frac{k}{40} w_2 (\theta_2^y) \\
& + \frac{9k}{80} w_2 (\theta_3^y) + \frac{7}{40} w_3 (\theta_1^x) - \frac{9}{80} w_3 (\theta_2^x) + \frac{1}{40} w_3 (\theta_3^x) + \frac{13k}{160} w_3 (\theta_1^y) - \frac{3k}{80} w_3 (\theta_2^y) \\
& - \frac{23k}{160} w_3 (\theta_3^y) - \frac{1}{40} a (\theta_1^x) (\theta_2^x) + \frac{1}{80} a (\theta_1^x) (\theta_3^x) + \frac{3k}{320} a (\theta_1^x) (\theta_1^y) \quad (12) \\
& - \frac{3k}{160} a (\theta_1^x) (\theta_2^y) - \frac{13k}{320} a (\theta_1^x) (\theta_3^y) + \frac{1}{120} a (\theta_2^x) (\theta_3^x) - \frac{13k}{320} a (\theta_2^x) (\theta_1^y) \\
& - \frac{k}{480} a (\theta_2^x) (\theta_2^y) + \frac{29k}{960} a (\theta_2^x) (\theta_3^y) - \frac{3k}{160} a (\theta_3^x) (\theta_1^y) - \frac{k}{240} a (\theta_3^x) (\theta_2^y) \\
& \left. - \frac{k}{480} a (\theta_3^x) (\theta_3^y) + \frac{k^2}{80} a (\theta_1^y) (\theta_2^y) - \frac{k^2}{40} a (\theta_1^y) (\theta_3^y) + \frac{k^2}{120} a (\theta_2^y) (\theta_3^y) \right].
\end{aligned}$$

The expressions for the λ values of the three other corner bars may be deduced from the expression for λ_{56} by rotating the cell through 180 degrees about one of the coordinate axes and by that bringing the bar under consideration into the location of the bar 5-6 in Fig. 2. The correspondence of the terms follows from the numbering of the displaced joints as presented in Table 3.

Table 3. Analogy in Parameters and Locations. Between λ_{56} (Eq. (12)) and λ Values of Three Other Corner Bars

λ_{56}	λ_{58}	λ_{76}	λ_{78}
w_1	$-w_2$	$-w_3$	w_4
w_2	$-w_1$	$-w_4$	w_3
w_3	$-w_4$	$-w_1$	w_2
θ_1^x	θ_2^x	$-\theta_3^x$	$-\theta_4^x$
θ_2^x	θ_1^x	$-\theta_4^x$	$-\theta_3^x$
θ_3^x	θ_4^x	$-\theta_1^x$	$-\theta_2^x$
θ_1^y	$-\theta_2^y$	θ_3^y	$-\theta_4^y$
θ_2^y	$-\theta_1^y$	θ_4^y	$-\theta_3^y$
θ_3^y	$-\theta_4^y$	θ_1^y	$-\theta_2^y$

Stability Matrix of Rectangular Bar Cells with $\mu = 1/3$

In models with $\mu = 1/3$ the corner bars are absent. The plane stress displacements of the nodes under unit loading are found in the usual way by the computer, and their knowledge allows to determine the length changes in the bars. Knowing these and the cross-section areas of the bars (Eq. 8), their stresses are easily found. Intermultiplication of bar stresses and the second derivatives of the λ values gives the terms of the stability matrix ($\mu = 1/3$) presented in Table 4.

Direct Stresses in Secondary Bars of Cells with Arbitrary μ

These members are stressed only in pure shear condition, and only when μ is distinct from $1/3$. Since the cell in its geometry and bar areas is symmetrical about the axes x and y through its centre, and the corner loads under pure shear antisymmetrical, the bar stresses F , F_1 and F_2 in the secondary bars must be also antisymmetrical, as is shown in Fig. 6. From equilibrium of mid-side joints it follows that

$$\frac{F}{\sin \alpha} = \frac{F_1}{\cos \alpha} = F_2. \tag{13}$$

Thus all F stresses in a particular cell are expressible through one of them.

Since the stresses F or F_1 in the two halves of each side bar are equal and opposite in sign the mean stresses S in side bars are independent of F and may be found from the nodal displacements and the total side bar areas, as has been explained for the cell with $\mu = 1/3$.

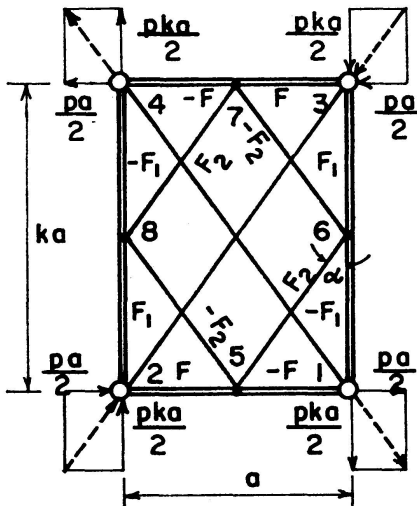


Fig. 6.

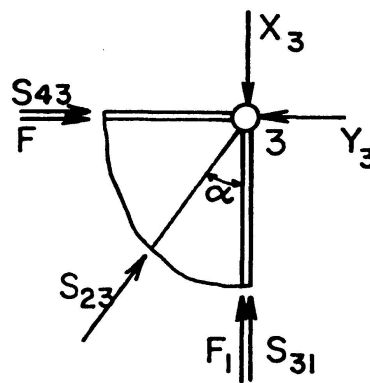


Fig. 7.

In general case of in-plane loads the stresses F differ from cell to cell. A convenient way to determine them is explained by reference to Fig. 7, representing the free body diagram of forces at one of the nodes of the cell, the node 3 in this case. The nodal forces X_3 and Y_3 are found as the products of the corresponding rows of the stiffness matrix and the vector of nodal displacements, and the stresses in the bars of the main system S_{43} , S_{23} and S_{31} - from the nodal displacement and the bar areas. Then F and F_1 follow from $\sum X = 0$ and $\sum Y = 0$, and F_2 - from Eq. (13).

The total contribution to the terms of the stability matrix by one of the side bars, such as the bar 4-3 (Fig. 5) is

$$(S_{47} - F) \frac{\partial^2 \lambda_{47}}{\partial \delta_m \partial \delta_n} + (S_{47} + F) \frac{\partial^2 \lambda_{73}}{\partial \delta_m \partial \delta_n} = S_{47} \left(\frac{\partial^2 \lambda_{43}}{\partial \delta_m \partial \delta_n} - F \frac{\partial^2 \lambda_{47}}{\partial \delta_m \partial \delta_n} + F \frac{\partial^2 \lambda_{73}}{\partial \delta_m \partial \delta_n} \right).$$

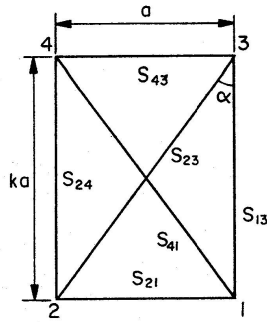
This means that the effects of the F and F_1 stresses in the halves of the secondary side bars are simply added on to the effects of the mean stresses (like S_{43}) in the stability matrix of Table 4. The contributions of the stress F are assembled in the auxiliary stability matrix of Table 5, which must be added to the main stability matrix, when Poisson's ratio of the model is distinct from $1/3$.

Table 4. Stability Matrix. Rectangular Bar Cell. $\mu = 1/3$

	w_1	θ_1^x	θ_1^y	w_2	θ_2^x	θ_2^y
w_1	$\frac{1.2S_{21}}{a} + \frac{1.2S_{13}}{ka}$ $+ \frac{1.2S_{41}}{a} \sin \alpha$					
θ_1^x	$-0.1S_{21}$ $-0.1S_{41} \sin \alpha$	$\frac{2aS_{21}}{15}$ $+ \frac{2aS_{41}}{15} \sin \alpha$				
θ_1^y	$0.1S_{13}$ $+0.1kS_{41} \sin \alpha$	$-\frac{2kaS_{41}}{15} \sin \alpha$	$\frac{2kaS_{13}}{15}$ $+ \frac{2k^2aS_{41}}{15} \sin \alpha$			
w_2	$-\frac{1.2S_{21}}{a}$	$0.1S_{21}$	0	$\frac{1.2S_{21}}{a} + \frac{1.2S_{24}}{ka}$ $+ \frac{1.2S_{23}}{a} \sin \alpha$		
θ_2^x	$-0.1S_{21}$	$-\frac{aS_{21}}{30}$	0	$0.1S_{21}$ $+0.1S_{23} \sin \alpha$	$\frac{2aS_{21}}{15}$ $+ \frac{2aS_{23}}{15} \sin \alpha$	
θ_2^y	0	0	0	$0.1S_{24}$ $+0.1kS_{23} \sin \alpha$	$\frac{2kaS_{23}}{15} \sin \alpha$	$\frac{2kaS_{24}}{15}$ $+ \frac{2k^2aS_{23}}{15} \sin \alpha$
w_3	$-\frac{1.2S_{13}}{ka}$	0	$-0.1S_{13}$	$-\frac{1.2S_{23}}{a} \sin \alpha$	$-0.1S_{23} \sin \alpha$	$-0.1kS_{23} \sin \alpha$
θ_3^x	0	0	0	$0.1S_{24} \sin \alpha$	$-\frac{aS_{23}}{30} \sin \alpha$	$-\frac{kaS_{23}}{30} \sin \alpha$
θ_3^y	$0.1S_{13}$	0	$-\frac{kaS_{13}}{30}$	$0.1kS_{24} \sin \alpha$	$-\frac{kaS_{23}}{30} \sin \alpha$	$-\frac{k^2aS_{23}}{30} \sin \alpha$
w_4	$-\frac{1.2S_{41}}{a} \sin \alpha$	$0.1S_{41} \sin \alpha$	$-0.1kS_{41} \sin \alpha$	$-\frac{1.2S_{24}}{ka}$	0	$-0.1S_{24}$
θ_4^x	$-0.1S_{41} \sin \alpha$	$-\frac{aS_{41}}{30} \sin \alpha$	$\frac{kaS_{41}}{30} \sin \alpha$	0	0	0
θ_4^y	$0.1kS_{41} \sin \alpha$	$\frac{kaS_{41}}{30} \sin \alpha$	$-\frac{k^2aS_{41}}{30} \sin \alpha$	$0.1S_{24}$	0	$-\frac{kaS_{24}}{30}$

w_3 θ_3^x θ_3^y w_4 θ_4^x θ_4^y

Symmetrical



$$\frac{S_{43}}{a} + \frac{1.2S_{13}}{ka}$$

$$\frac{1.2S_{23}}{a} \sin \alpha$$

$$0.1S_{43}$$

$$0.1S_{23} \sin \alpha$$

$$\frac{2aS_{43}}{15}$$

$$+ \frac{2aS_{23}}{15} \sin \alpha$$

$$0.1S_{13}$$

$$0.1kS_{23} \sin \alpha$$

$$\frac{2kaS_{23}}{15} \sin \alpha$$

$$\frac{2kaS_{13}}{15}$$

$$+ \frac{2k^2aS_{23}}{15} \sin \alpha$$

$$-\frac{1.2S_{43}}{a}$$

$$0.1S_{43}$$

$$0$$

$$\frac{1.2S_{43}}{a} + \frac{1.2S_{24}}{ka}$$

$$+ \frac{1.2S_{41}}{a} \sin \alpha$$

$$-0.1S_{43}$$

$$-\frac{aS_{43}}{30}$$

$$0$$

$$0.1S_{43}$$

$$+ 0.1S_{41} \sin \alpha$$

$$\frac{2aS_{43}}{15}$$

$$+ \frac{2aS_{41}}{15} \sin \alpha$$

$$0$$

$$0$$

$$0$$

$$-0.1S_{24}$$

$$-0.1kS_{41} \sin \alpha$$

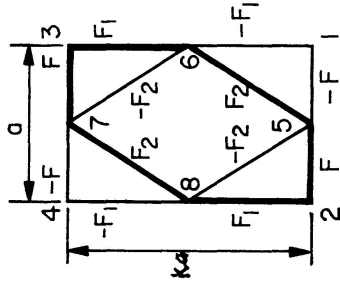
$$-\frac{2kaS_{41}}{15} \sin \alpha$$

$$\frac{2kaS_{24}}{15}$$

$$+ \frac{2k^2aS_{41}}{15} \sin \alpha$$

Table 5. Addition to Stability Matrix. Rectangular Bar Cell. Any μ .

	w_1	θ_1^x	θ_1^y	w_2	θ_2^x	θ_2^y	w_3	θ_3^x	θ_3^y	w_4	θ_4^x	θ_4^y
w_1	$-\frac{0.825F}{a}$											
θ_1^x		$\frac{7aF}{120}$										
θ_1^y			$\frac{7k^2aF}{120}$									
w_2				$\frac{0.825F}{a}$								
θ_2^x					$\frac{7aF}{120}$							
θ_2^y						$\frac{7k^2aF}{120}$						
w_3							$\frac{0.825F}{a}$					
θ_3^x								$\frac{7aF}{120}$				
θ_3^y									$\frac{7k^2aF}{120}$			
w_4										$\frac{0.825F}{a}$		
θ_4^x											$\frac{7aF}{120}$	
θ_4^y												$\frac{7k^2aF}{120}$



Symmetrical

Bar Stiffnesses

A word of caution concerning the proportions of the bar cells is in order. Examination of expressions of extensional bar stiffnesses, Eq. (8), shows that the cross-section area of the longer side bar becomes zero, i. e., the bar vanishes, when $\mu k^2 = 1$. With the longer side bars absent the plate model ceases to be a structure and becomes a mechanism. Cells of this kind are inadmissible. When the cell's aspect ratio $k > \sqrt{2}$, the quantity μk^2 may exceed unity making the stiffnesses of the longer side bars, both extensional and flexural, negative. The torsional stiffnesses of side bars become also negative when $\mu > 1/3$.

Experience shows that models with negative bar stiffnesses result in lower precision, even though the results improve on reduction of the mesh size. The lack of precision appears to be associated with the stiffness matrix and not the stability matrix. For this reason it is recommended that the cells are so proportioned that the quantity μk^2 be kept under a value lower than unity, such as 0.9. Should a high aspect ratio k become imperative a substitute problem involving a lower μ may be solved. The effect of such substitution on the value of critical load is not great and may sometimes be corrected on the basis of theoretical considerations.

Examples

The examples considered involve rectangular plates in the following conditions of loading:

- a) Uniform compression in one direction.
- b) Uniform and equal compressions in two perpendicular directions.
- c) Uniform shear in the direction of edges.

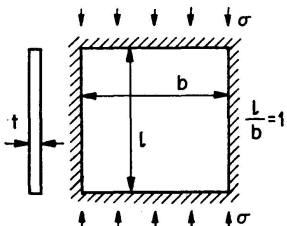
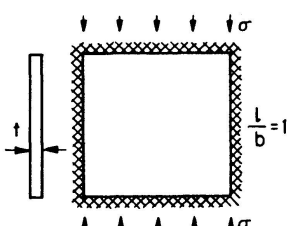
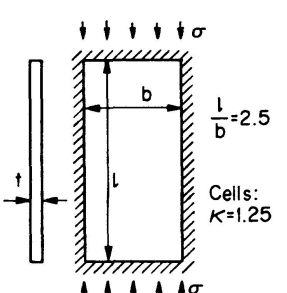
With regard to the plane stress action the plates are assumed free at the edges, while in their flexural action they are considered either simply supported or fixed at the edges.

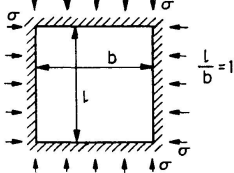
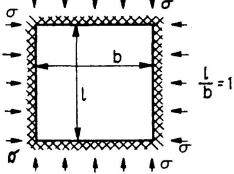
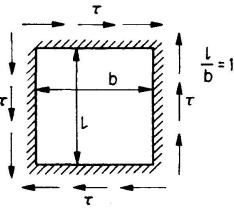
The critical unit stress, compression or shear, depending on the problem, is given by the formula

$$\delta_{cr} \text{ (or } \tau_{cr}) = \beta \frac{\pi^2 D}{b^2 t}. \quad (14)$$

Here b is the dimension of the plate in the direction normal to the direction of compression in case a), and in either of the two perpendicular directions in cases b) and c); t is the plate thickness; $D = \frac{E t^3}{12(1-\mu^2)}$ is the elastic constant and β the parameter whose exact values, stated in references [1], [4] and [5] depend of the type of loading, the flexural edge restraints and the ratio of the sides of the plate.

Table 6. Critical Buckling Stresses in Plates. % Errors of Finite Element Solutions. Bar and No-Bar Cells.

Problem	μ	μk^2	Bar or No-bar	% Error		
				Model Mesh		
				3 × 3	4 × 4	6 × 6
 <p>Exact $\beta = 4.00$</p>	0.3	0.3	No-Bar	-8.88	-5.75	-2.80
	0.3	0.3	Bar	-10.0	-5.75	-2.75
	0.1	0.1	Bar	-9.5	-5.5	-1.75
	0.45	0.45	Bar	-10.2	-6.5	-3.0
 <p>Exact $\beta = 10.07$</p>	0.3	0.3	No-Bar	—	-7.80	-4.56
	0.3	0.3	Bar	-13.0	-8.60	-5.17
	0.1	0.1	Bar	-13.1	-8.60	-4.37
	0.45	0.45	Bar	-13.1	-9.0	-5.17
 <p>Exact $\beta = 4.133$</p>				3 × 6	4 × 8	6 × 12
	0.3	0.469	No-Bar	—	-7.10	-3.75
	0.3	0.469	Bar	-5.0	-4.05	-2.82
	0.1	0.156	Bar	-11.2	-8.15	-5.10
	0.45	0.703	Bar	-1.55	-1.97	-1.20
As directly above, except $l/b = k = 1.5$ Exact $\beta = 4.339$	0.1	0.225	Bar	4 × 4	6 × 6	8 × 8
	0.333	0.75	Bar	-8.8	-6.13	-4.4
	0.45	1.012	Bar	-2.59	-3.1	-2.58
			Bar	-49.0	-8.84	-3.23
As directly above, except $l/b = k = 1.75$ Exact $\beta = 4.071$	0.1	0.306	Bar	4 × 4	6 × 6	8 × 8
	0.333	1.025	Bar	-10.0	-7.6	-5.04
	0.45	1.375	Bar	-3.26	-4.7	-3.82
			Bar	-85.4	-64.6	-40.4

Problem	μ	Bar or No-Bar	% Error		
			Model Mesh		
			3 × 3	4 × 4	6 × 6
 <p>Exact $\beta = 2.00$</p>	0.3	No-Bar	-12.95	-5.5	-2.75
	0.3	Bar	-9.3	-5.84	-2.66
	0.1	Bar	-8.96	-5.2	-2.32
	0.45	Bar	-10.2	-6.5	-3.04
 <p>Exact $\beta = 5.315$</p>	0.3	No-Bar	—	-6.38	-4.46
	0.3	Bar	-16.0	-8.8	-4.9
	0.1	Bar	-12.9	-8.7	-4.57
	0.45	Bar	-11.4	-8.76	-5.26
 <p>Exact $\beta = 9.34$</p>	0.3	No-Bar	-12.1	-10.2	-6.47
	0.3	Bar	-22.0	-11.6	-6.42
	0.1	Bar	-17.95	-10.3	-6.07
	0.45	Bar	-32.6	-15.1	-6.73
<p>As directly above, except $l/b = k = 1.25$</p> <p>Exact $\beta = 7.71$</p>	0.3	No-Bar	—	-9.92	-6.00
	0.3	Bar	-23.1	-11.8	-5.95
	0.1	Bar	-18.5	-10.35	-5.52
	0.45	Bar	-34.8	-15.9	-6.3



Edges Simply Supported in Flexure



Edges Clamped in Flexure

The results of solution are much similar in all types of loading, and for the reason of economy of space only a few of them are presented in Table 6, in the form of % errors of the coefficient β found by the bar and the no-bar cells, with the minus sign indicating a deficiency in the approximate values.

Here are some observations on the results:

1. When the bar stiffnesses are positive the results of the bar cell solutions are good and closely comparable to the ones obtained with the no-bar cells.
2. The approximate values are lower than the exact values.
3. On making the mesh finer, while retaining the same aspect ratio of cells, the precision usually improves somewhat faster than in the ratio of the linear dimensions of cells.
4. The precision does not seem to be influenced by the type of loading or the manner of edge restraints.
5. In the use of oblong cells when $\mu k^2 > 1$ the results are irregular and at times very inaccurate, but they usually improve as the mesh becomes finer.
6. Within the limits $\mu k^2 < 1$ the results seem to become less precise as k is increased.

Conclusion

Bar Cells and No-Bar Cells in Stability Analysis

In spite of basic similarities of the procedures used with the bar and the no-bar cells; there are significant distinctions between the two, which it is advisable to have clearly stated.

1. The loss of precision in case of bar cells with high values of μk^2 is an important weakness. This defect however may be eliminated either by suitably proportioned cells or by hybrid solutions involving no-bar cell stiffness matrix and bar cell stability matrix.
2. The stiffness and stability matrices used in the no-bar cell solutions (1) are theoretically deficient because of the lack of slope conformity along the edges of cells. The error arising from this source in uniform and some other regular, loading conditions is apparently small. What this error may be in more complicated loading conditions is uncertain. The bar cells on the other hand are fully conformable at the nodes, the only locations where the adjacent cells meet.
3. The bar cell solutions presented here contains in explicit form all the necessary information and data required in stability analysis of any arbitrarily loaded rectangular plate. The necessary cell stability matrices Tables 4 and 5, cover all kinds of loading described by the stresses S . On the other hand the no-bar cell analysis requires a multiplicity of stability matrices, only a few of which, applicable to certain simple types of cell loading, are given explicitly. The complete generality of the proposed bar cell stability matrix makes it superior to its no-bar cell counterpart.

Notation

A, A', A''	cross-sectional areas of short side-bars of cells, total, primary, secondary.
A_1, A'_1, A''_1	cross-sectional areas of longer side bars of cells, total, primary, secondary.
A_2, A_3	cross-sectional areas of diagonal and corner bars.
D	elastic flexural constant of plate.
E	modulus of elasticity.
F, F_1, F_2	additional stresses in members of secondary bar system.
$[K], [K]_m$	stiffness matrices of cell and of model.
$[K_s], [K_s]_m$	stability matrices of cell and of model.
P	plane stress loads.
S	with and without subscripts, bar stresses, direct.
T	increment of total energy of model on buckling.
U	increment of energy of deformation on buckling.
V	increment of potential energy on buckling.
X, Y	components of forces.
X, Y	with subscripts – members of plane stress stiffness matrix.
a	smaller dimension of cell.
b	dimension of plate along y axis.
f	critical intensity of load.
k	aspect ratio of cell.
l	length.
t	thickness of plate.
w	deflection of plate and of bar.
w	with subscripts – node and joint displacements.
x, y	rectangular coordinates.
α	angle of diagonal bar.
β	parameter defining critical load.
ϵ	displacement of point of application of load.
λ, λ	with subscripts – shortening of projection of bar length caused by flexure.
$\delta, \delta_m, \delta_n$	movements of the nodes.
σ_{cr}	critical normal unit stress.
τ_{cr}	critical unit shear stress.
θ^x, θ^y	with and without subscripts – nodal rotations.

Acknowledgement

The research forming the basis of this paper was conducted with financial assistance of the National Research Council of Canada.

References

1. KAPUR, K. K. and HARTZ, B. J.: Stability of Plates Using Finite Element Method. Jour. Eng. Mech. Div., ASCE, E.M. 2, Vol. 92, April, 1966.
2. HRENNIKOFF, A.: Solution of Problems of Elasticity by the Framework Method. Jour. of Applied Mechanics, ASME, Vol. 63, December, 1941.
3. YETTRAM, A. L. and HUSEIN, H. M.: Grid Framework Method for Plates in Bending. Jour. of Eng. Mech. Div., ASCE, Vol. 91, June 1965.
4. TURNER, M. J., CLOUGH, R. W., MARTIN, H. C. and TOPP, L. J.: Stiffness and Deflection Analysis of Complex Structures. Jour. of the Aeronautical Sciences, Vol. 23, No. 9, September 1956.
5. TIMOSHENKO, S. P. and GERE, J. M.: Theory of Elastic Stability. McGraw-Hill Book Co. Inc. New York, N.Y. 1961.

Summary

The finite element method, making use of rectangular bar cells, is applied to the problem of stability of rectangular plates under the action of in-plane loads. The method is similar in principle to the method involving no-bar cells, proposed by K. K. KAPUR and B. J. HARTZ [1]. The application of the method is demonstrated on several examples, whose exact solutions are available. Investigation is also made of the effects of bar stiffnesses on precision under the influence of the aspect ratio of cells and the Poisson's ratio of the material.

Résumé

La méthode des éléments finis qui utilise des éléments de barre rectangulaires est appliquée au problème de la stabilité de dalles rectangulaires sous l'influence de charges planes. Cette méthode est en principe similaire à celle qui travaille avec des éléments non-barres, proposée par K. K. Kapur et B. J. Hartz. L'application de la méthode est montrée dans plusieurs exemples dont les solutions exactes sont connues. Des recherches sont faites sur l'effet de la rigidité de la barre, en particulier sous l'influence de la disposition des éléments et du coefficient de Poisson.

Zusammenfassung

Die Methode der finiten Elemente, welche mit rechteckigen Stabelementen arbeitet, wird auf das Problem der Festigkeit rechteckiger Platten unter der Wirkung ebener Lasten angewandt. Diese Methode ist im Prinzip ähnlich wie jene, welche mit Nicht-Stab-Elementen arbeitet und die von K. K. Kapur und B. J. Hartz vorgeschlagen wird. Die Anwendung der Methode wird an zahlreichen Beispielen gezeigt, deren genaue Lösungen vorhanden sind. Untersucht wurden auch die Auswirkungen der Elementverteilung und der Poisson'schen Zahl auf die Stabsteifigkeit.